THE JOURNAL OF PHYSICAL CHEMISTRY B

ARTICLE

pubs.acs.org/JPCB

Water Self-Diffusion in Glassy and Liquid Maltose Measured by Raman Microscopy and NMR

Lei Zhu,[†] Ting Cai,[†] Jun Huang,[†,§] Thomas C. Stringfellow,[†] Mark Wall,[‡] and Lian Yu*[,†]

[†]School of Pharmacy and Department of Chemistry, University of Wisconsin-Madison, 777 Highland Avenue, Madison, Wisconsin 53706, United States

[‡]Thermo Fisher Scientific, 5225 Verona Road, Madison, Wisconsin 53711, United States

ABSTRACT: Raman microscopy and isotope labeling have been used for the first time to measure water self-diffusion in carbohydrate glasses. Together with pulsed-gradient stimulated-echo NMR, this method yielded the self-diffusion coefficients of water in amorphous maltose over 8 orders of magnitude, from the liquid to the glassy state. There are consistencies and major differences between our data and those obtained by evaporative drying. Water diffusion is remarkably fast in maltose glasses, decouples from maltose diffusion, and is not strongly affected by the glass transition.

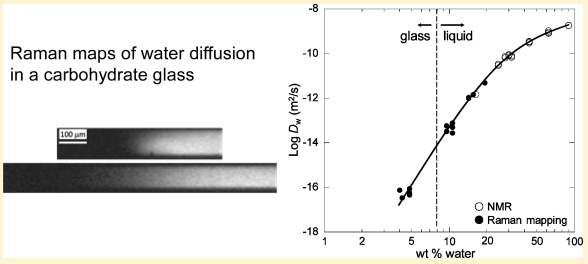

INTRODUCTION

Amorphous carbohydrates are common ingredients of food and pharmaceutical products and matrices for preserving proteins and organisms. The mobility of water molecules in amorphous carbohydrates is of interest because hydration can accelerate physical and chemical changes. Among the various measures of water mobility, translational diffusion has received experimental[1−8] and theoretical attention.[3,4,9−11] Of particular interest in this context is the proposed mechanism of translational jumps for water diffusion in carbohydrates[4,9,10] and the possibility of non-Fickian kinetics in glassy systems.[12] Understanding water diffusion in carbohydrates could benefit the research of other materials whose hydration has scientific and technological implications, including polymers[12] and silicate glasses.[13]

Carbohydrate−water systems of technological importance differ greatly in molecular mobility, ranging from solutions of relatively low viscosities to solutions so concentrated or so cold that they solidify to glasses. To measure water diffusion in low-viscosity solutions, NMR[1−4] and quasi-elastic neutron scattering[5,9] have been the principal techniques, yielding water diffusion coefficients D_w down to ca. 10^{-12} m^2/s. To measure slower water diffusion, the standard method has been evaporative drying.[6−8] Studies using this technique have found that water diffusion remains fast in the glassy state, with $D_w \approx 10^{-13}-10^{-14}$ m^2/s near the glass transition temperature T_g. For the water−maltose system, a complex dependence of D_w on water concentration has been reported in the glass transition region.[6,7]

In this study, we tested a new method, Raman microscopy combined with isotope labeling, for measuring water diffusion in carbohydrate glasses. Despite its simplicity and convenience, the evaporative drying method encounters complications when D_w depends strongly on concentration.[12] During evaporative drying, a sample's surface is drier than its interior; the measured D_w is a mean diffusion coefficient averaged over a range of water concentrations. Previous studies have found strong concentration dependence of the rate of water diffusion in carbohydrates.[6,7] For these materials, it would be more rigorous to measure diffusion in a medium of constant water concentration. In our method, an interface is formed between a material containing H_2O and the same material containing D_2O of identical concentration; the broadening of the interface is monitored over time by Raman microscopy, a technique of chemical analysis at submicrometer resolution.[14,15] This method could provide independent data on water diffusion in carbohydrates and be relevant for measuring water diffusion in other materials whose hydration has scientific and technological interest.

We report here self-diffusion coefficients of water in amorphous maltose measured with Raman microscopy and NMR in the range of 10^{-9} to 10^{-17} m^2/s, from the liquid to the glassy state. To our knowledge, this is the largest range over which the water diffusion coefficient has been measured for a single system. We find consistency and significant differences between our data and data obtained by evaporative drying.[6,7] Our data show that water diffusion is remarkably fast in maltose glasses, decouples from maltose diffusion, and is not strongly affected by the glass transition. These results are relevant for understanding water diffusion in amorphous carbohydrates and predicting the stability of food, drugs, and biomaterials. This study also demonstrates the utility of Raman microscopy for measuring water diffusion in solids.

EXPERIMENTAL SECTION

Maltose monohydrate and D_2O were purchased from Sigma-Aldrich (St. Louis, MO) and used as received. H_2O used was Milli-Q water. To prepare a sample for diffusion measurement by NMR, maltose monohydrate was dissolved in H_2O at the desired

Received: March 21, 2011
Revised: April 1, 2011
Published: April 14, 2011

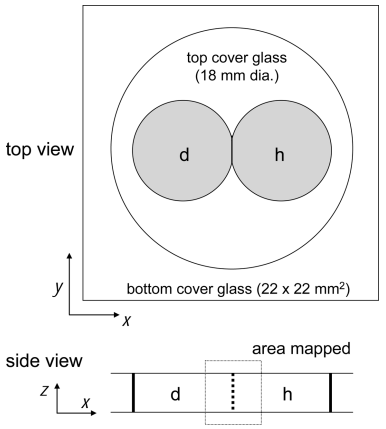

Figure 1. Experimental setup for measuring water self-diffusion by Raman microscopy and isotope labeling. h: H_2O-maltose solution; d: D_2O-maltose solution of identical concentration. Liquid thickness was 80−130 μm.

concentration and transferred into an NMR tube. Solutions of lower water concentrations (<20 wt %) were warmed before transfer. After NMR analysis, the sample in the tube was analyzed by KF titration (see below) to determine its water concentration. To prepare samples for Raman mapping, a 50 wt % maltose−water solution was first prepared by dissolving maltose monohydrate in H_2O or D_2O at 333 K. The solution was transferred to an aluminum weighing boat and dried in vacuum at 373 K to reach the desired water concentration. We noticed that the surface of the sample was drier than the interior and used only the material from the interior for diffusion studies. The interior water concentration was determined by KF titration.

For a Raman mapping experiment, a drop of maltose−H_2O solution and a drop of maltose−D_2O solution of identical concentration were placed side by side on a cover glass (Figure 1). A second cover glass was placed over the droplets, and the assembly was heated to ca. 40 K above the liquids' T_g. Once contact was made between the two liquids, the assembly was cooled to room temperature (296 ± 1 K), at which diffusion was measured. The liquid layer thus prepared was 80−130 μm, which did not change significantly during measurement.

Raman Microscopy. Raman microscopy was performed with a Thermo Scientific DXR Raman microscope. The spectrometer has no moving parts and captures the spectral range 50−3500 cm^{-1} in one exposure at 5 cm^{-1} resolution. The design allows relatively fast data acquisition required for mapping. Raman maps were acquired by collecting spectra at various positions with the aid of a computer-controlled translational stage. The smallest step size was 1 μm along the horizontal (x and y) directions and 2 μm in the vertical (z) direction. A 10 mW 532 nm laser was used for excitation. Background, fluorescence, and white-light corrections were applied. Raman spectra were collected through a 50× dry objective and a 25 μm pinhole at an image plane to provide the confocal condition to improve spatial resolution.

Analysis of Raman Maps to Obtain Diffusion Coefficients. The intensities of characteristic Raman bands of the protio and deuterio materials were used to determine the spatial distributions of diffusing species as a function of time. With our measurement geometry (Figure 1), the sample can be treated as two semi-infinite slabs that contact in the yz plane ($x = 0$). If the initial interface is sharp relative to the instrument's spatial resolution, the intensity of the Raman signal of the h or d species as the laser scans along x across the interface is the convolution of a step function and the instrument's point-spread function, $g(x)$. If $g(x)$ has a Gaussian form, $g(x) = [(2\pi)^{0.5}\sigma_x]^{-1} \exp[-x^2/(2\sigma_x^2)]$, the result is an error function:

$$I_h(x) = I_{h0}\{1 + \mathrm{erf}[x/(2^{0.5}\sigma)]\}/2 \quad (1)$$

$$I_d(x) = I_{d0}\{1 - \mathrm{erf}[x/(2^{0.5}\sigma)]\}/2 \quad (2)$$

where I_{h0} (I_{d0}) is the Raman intensity of the pure h (d) species, and $\sigma = \sigma_x$ is the interfacial width that characterizes the instrument's spatial resolution. For an interface broadened by Fickian diffusion, σ increases according to

$$\sigma^2 = \sigma_x^2 + 2Dt \quad (3)$$

where D is the mutual diffusion coefficient, and t is diffusion time. If the difference is neglected between the diffusivities of the protio and deuterio species, D is the self-diffusion coefficient.

Our procedure for determining D from Raman maps is (i) Fit $I_h(x)$ and $I_d(x)$ to eqs 1 and 2 to obtain σ after each diffusion time t; and (ii) plot σ^2 against t. Linearity of the plot verifies Fickian diffusion, whose slope gives $2D$ and whose intercept, σ_x^2.

The model above assumes that the interfacial width at $t = 0$ is sharp relative to the instrument's resolution, σ_x; that is, we assume that the interfacial broadening is minimal during the brief contact of the h and d liquids at a relatively high temperature in sample preparation (Figure 1). This assumption was often found valid on inspecting the Raman maps. Even if the initial interfacial width σ_{D0} is not negligible relative to σ_x, our procedure would still be justified because σ_{D0} is a constant for a given sample, and eq 3 still has the form σ^2 = constant + $2Dt$, where the new constant is $(\sigma_x^2 + \sigma_{D0}^2)$.

Pulsed-Gradient Stimulated-Echo NMR. Pulsed-gradient stimulated-echo NMR was performed on a Varian UNITY-INOVA spectrometer at 11.74 T (500 MHz proton frequency) using either a 5 mm inverse-detection Varian HCX probe or a 5 mm direct-detection Nalorac QN probe, both equipped with a z-axis gradient coil. Unless otherwise indicated, measurements were made with the sample temperature regulated at 298 K.

Water diffusion was measured in H_2O-maltose solutions, rather than D_2O−maltose solutions, to obtain results that can be directly compared with those obtained via other measurement methods that utilized H_2O and to circumvent complications of data interpretation due to statistical variations in the molecular masses of maltose and water arising from H/D exchange. Using H_2O rather than D_2O requires that NMR measurements be made without utilizing the field−frequency lock mechanism. Owing to good magnet stability and typical data acquisition times of less than four minutes, running "unlocked" presents no inherent compromise to data quality or analysis. Another operational consequence, due to the excessive ^1H concentration, was the necessity to use an external attenuator to enable 90-degree RF pulses without concomitantly exceeding the 16-bit capacity of the analog-to-digital converter. These operational adjustments are standard procedure when using protonated, rather than deuterated, solvents.

The pulsed-gradient stimulated-echo method of Tanner[16,17] was used to measure translational diffusion coefficients via the

relationship

$$A(G_z) = A_0 \exp[-D(\gamma\delta G_z)^2(\Delta - \delta/3)] \qquad (4)$$

Here A represents the resonance amplitude (measured as either the integrated area or the intensity of the resonance signal), A_0 is the initial amplitude, γ is the magnetogyric ratio of the observed nuclide (^{1}H), D is the diffusion coefficient, δ is the duration of the gradient pulses, Δ is the delay between the encoding and decoding gradient pulses, and G_z is the magnitude of the applied gradient.

Values of δ = 2.0 ms and Δ = 30.0 ms were typically used for calibration measurements using H_2O/D_2O. For water−maltose systems, optimal values for δ and Δ depend upon the solution concentration: larger values become increasingly necessary with decreasing water content, which corresponds to a concomitant increase in solution viscosity. Due to operational limits, values for δ did not exceed 4 ms; consequently, the parameter Δ was primarily optimized to attain sufficient attenuation of the resonance amplitude. The following experimental pairs of δ and Δ values illustrate: δ = 2.0 ms, Δ = 30.0 ms (90.4 wt % water); δ = 3.0 ms, Δ = 40.0 ms (43.5 wt % water); δ = 4.0 ms, Δ = 140.0 ms (31.6 wt % water); δ = 4.0 ms, Δ = 300.0 ms (24.7 wt % water); δ = 4.0 ms, Δ = 2500 ms (16.2 wt % water). Measured diffusion coefficients were found to be essentially invariant to Δ for samples at higher water concentrations; however, a slight dependence on Δ was observed at lower concentrations. For example, at 25 wt % water concentration, an approximately 30% decrease in D_w was observed upon changing Δ from 160 to 300 ms. This phenomenon could be associated with increasingly nonexponential dynamics as liquids approach the glass transition temperature. The effect is relatively small, however, for our analysis of water diffusion coefficients over several orders of magnitude.

The independent variable G_z was arrayed as 18 values in equal increments, for both calibration and water/maltose measurements, ranging between approximately 2 and 62 G/cm (0.02−0.62 T/m). These parameter values provided (*i*) stable and reproducible gradient pulse amplitudes; (*ii*) adequate time, via Δ, for loss of initial spatial phase encoding through translational diffusion; and (*iii*) sufficient range of gradient strength, G_z, to ensure attenuation of the resonance to approximately 10% or less of its initial amplitude over the extent of the acquisition array. All measurements utilized a recycle time large enough to allow complete recovery of longitudinal relaxation between transient acquisitions.

Calibration experiments were performed to determine the final instrument response to the digital-to-analog conversion (DAC) values, g, used as the primary independent variable, and thus determine the resultant gradient strengths, G_z. These experiments used a sample of H_2O/D_2O in the ratio 1/99, for which the diffusion coefficient was taken as 1.90×10^{-9} m^2 s^{-1} at 298 K.[18] Each calibration experiment was executed using the above-indicated sample and acquisition parameters; postacquisition processing included phase and baseline correction prior to integration of the HOD resonance. The peak-area data were then analyzed via nonlinear fit[19] to eq 4 as a function of g to simultaneously obtain A_0 and κ ($G_z = g\kappa$) using the known diffusion coefficient. At least two calibration experiments were performed for every session of sample measurements. Typical values thus determined for κ were 0.001868 G/cm per DAC unit; standard deviations were on the order of 10^{-6}, and a variation of ±0.000020 represents a 95% confidence range for κ.

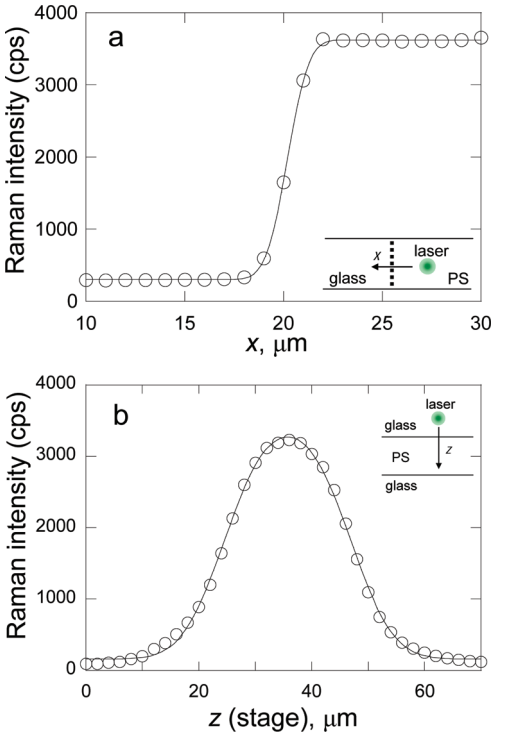

Figure 2. (a) Raman intensity of PS across a vertical PS/glass interface (inset). Fitting the profile to eq 1 (curve) yields σ_x = 0.84 μm. (b) Raman intensity of PS across two horizontal PS/glass interfaces (inset). The z coordinate is in the unit of stage travel. Fitting the profile to eq 1 modified for two adjacent interfaces (curve) yielded σ_z = 5.9 μm or 5.9 × 1.59 = 9.4 μm in actual distance in PS (n = 1.59).

For diffusion measurements of water/maltose samples, acquisition parameters were set, and data processing was carried out as described above. The ^{1}H resonance of water was integrated and/or its intensity (height) measured for subsequent analysis of the $A(G_z)$ data, which were similarly fit to eq 4 to obtain both A_0 and D as best-fit parameters. More pronounced at higher water concentrations, the maltose anomeric proton resonances (especially the β anomer resonance at 4.65 ppm) overlap with the tail of the water resonance, making an undesirable contribution to the integrated area of the water resonance; consequently, the water peak intensity was used as the dependent variable in those cases for which it appeared to more accurately represent the true attenuation of the water resonance.

Karl Fisher Titration. Karl Fisher titration was performed with a Metrohm 831 KF Coulometer to determine water concentration. A sample to be analyzed was placed in a dry vial. A known amount of predried KF reagent (Hydranal − Coulomat AG) was drawn directly from an equilibrated reaction vessel and added to the vial. The vial was sealed with a rubber stopper and aluminum crimp and shaken to dissolve the solid. The solution was injected back to the KF reaction vessel to determine its water concentration. In a blank run, the procedure was repeated with an empty vial and the amount of moisture measured was subtracted from that measured for an actual sample. The KF method was validated using crystalline maltose monohydrate for which the water content was independently determined by weight loss on vacuum drying at 393 K. For this material, the KF method reported 4.1 wt % H_2O, whereas drying yielded 4.5 wt % H_2O.

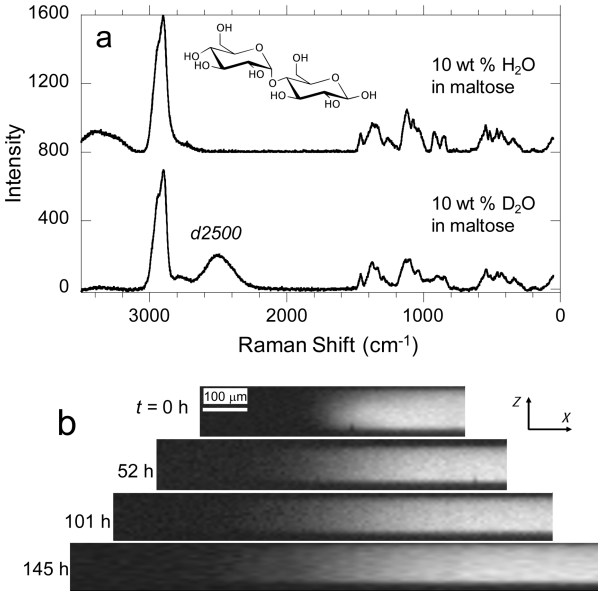

Figure 3. (a) Raman spectra of 10 wt % H_2O in maltose and 10 wt % D_2O in maltose. Inset is the structure of maltose (β anomer). (b) Raman xz maps of the OD group at the interface between the two liquids in (a) at 296 K. The peak d2500 was used to construct these maps. Brightness indicates Raman intensity (bright = high; dark = low).

Differential Scanning Calorimetry (DSC). DSC was performed with a TA Instruments DSC Q2000 at 10 K/min in hermetically sealed Al pans under 50 mL/min N_2 purge. DSC was used to measure the glass transition temperatures (T_g) of maltose-water containing 4−15 wt % water.

RESULTS

Spatial Resolution of the Raman Microscope. The spatial resolution of a Raman microscope depends on the microscope's objective, the refractive index of the medium, scan direction (lateral or vertical), laser wavelength, and depth of focus.[14,15] For convenience, we used polystyrene (PS, M_w = 1780), a strong Raman scatterer, as the test material; the similar indices of refraction of PS (1.59) and maltose monohydrate (1.55)[20] mean that the microscope resolution determined with PS applies to maltose−water systems at high concentrations. To determine the lateral (x) resolution, a vertical interface was created between PS and a silicate glass, two media of similar indexes of refraction (Figure 2a, inset). To prepare this sample, a glass spacer 150 μm thick was placed between two microscope coverslips; a PS sample was heated so that it flowed into contact with the spacer. Figure 2 shows the intensity (height) of the PS Raman peak at 1000 cm^{-1} as the laser spot traveled normal to the interface from PS to the glass. Fitting the profile to eq 1 yielded σ = 0.84 μm, which we assign as the instrument's resolution along x, σ_x.

To determine the depth (z) resolution, a layer of PS liquid was formed between two cover glasses and scanned along z. The thickness of the liquid was controlled using two parallel glass fibers (diameter ca. 30 μm). Figure 2b shows the Raman intensity versus z (distance traveled by the microscope stage). Fitting the profile as the convolution of a square function of PS concentration and a Gaussian instrumental function yielded σ_z = 5.9 μm. Because the laser traveled in a medium (PS or glass) with an index of refraction of 1.59, the actual z resolution is 5.9 × 1.59 = 9.4 μm. The fitting also yields the thickness of this sample: 23 μm as the distance of stage travel or 23 × 1.59 = 36 μm for the actual thickness. The latter agrees with the diameter of the fiber spacers.

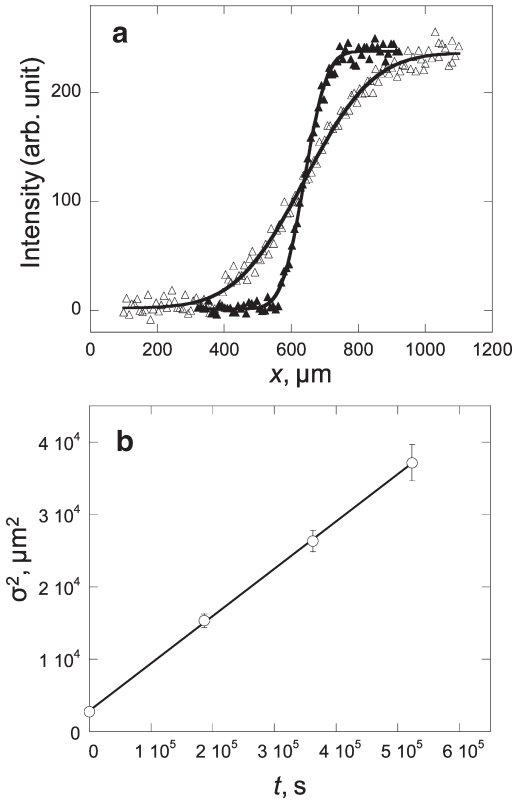

Figure 4. (a) x-Profiles of OD concentration in the sample in Figure 3 at time zero (solid symbol) and after 145 h (open symbol) at 296 K. (b) Square of interfacial width vs time.

Water Diffusion in Amorphous Maltose. Figure 3 shows representative data collected to measure water self-diffusion in maltose. In this experiment, an interface was formed between a maltose−H_2O solution and a maltose−D_2O solution, each containing 10 wt % water, as illustrated in Figure 1. Figure 3a shows the Raman spectra of the two solutions. The 2500 cm^{-1} peak in the maltose−D_2O spectrum was used to map the spatial distribution of the OD group as a function of time at 296 ± 1 K (Figure 3b). These maps were made in an xz plane with the x direction being perpendicular to the h/d interface and the z direction being parallel to the h/d interface. These maps show significant diffusion of the OD group over time, and no significant change of the sample thickness. We attribute the movement of the OD group to water diffusion. Because the concentration of water (in all isotopic forms) was uniform throughout the sample, the diffusion observed here is reasonably considered the self-diffusion of water. We observed similar diffusion of the OH group by following the 3400 cm^{-1} peak, but the OH maps were substantially noisier than the OD maps.

Figure 4a shows the profiles of the OD concentration along x. Only the results from the first and the last time point are shown. Fitting the profile at each time point to eq 1 yielded the interfacial widths shown in Figure 4b. The data are plotted in the format σ^2 versus t. The linearity of this plot indicates Fickian diffusion and its slope yields the diffusion coefficient for water D_w in the maltose−water solution, which in this case is 3.3 × 10^{-14} m^2/s.

dx.doi.org/10.1021/jp202663r |J. Phys. Chem. B 2011, 115, 5849–5855

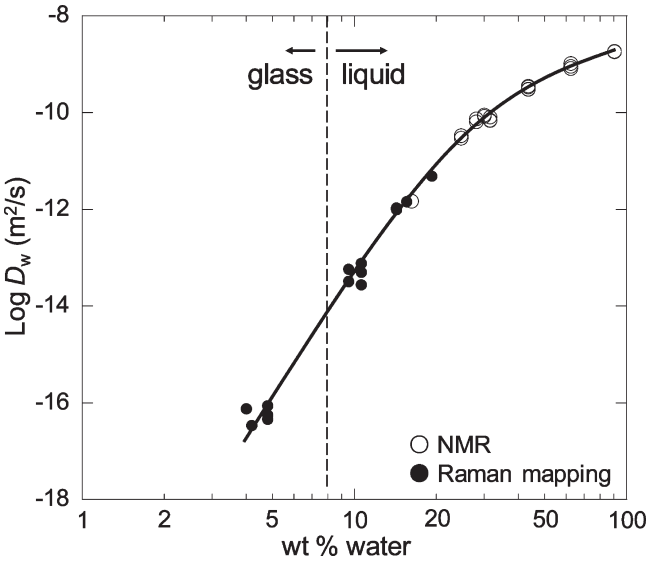

Figure 5. Water diffusion coefficient D_w in a water−maltose solution as a function of water concentration. Raman measurements at 296 ± 1 K. NMR measurements at 298.0 ± 0.5 K.

In this study, Raman microscopy was used to measure water diffusion in amorphous maltose containing 5−20 wt % water, in which D_w was found to be from 10^{-17} to 10^{-11} m^2/s. Fickian kinetics was observed for all maltose−water systems studied, in both the liquid and the glassy state. This finding is consistent with the conclusion of the previous evaporative-drying studies.[6−8] NMR was used to measure larger water diffusion coefficients in the range 10^{-12} to 10^{-9} m^2/s (for 15−100 wt % water). Together, these two methods cover 8 orders of magnitude change in D (Figure 5). There was a slight difference between the temperatures of the two measurements: 296 ± 1 K for Raman microscopy and 298.0 ± 0.5 K for NMR. This temperature difference has been neglected given the relatively small changes it causes on water diffusion coefficient compared to the much greater changes caused by changing water concentration. For samples of similar concentrations (15 wt % water), the two techniques yielded similar results, indicating the validity of the Raman mapping method for measuring slow water diffusion in amorphous maltose.

Other Properties of the Systems Studied: T_g and Anomeric Ratio. Figure 6 shows the glass transition temperatures T_g of the maltose−water solution used in this work. According to our data, maltose−water solutions containing less than 8 wt % water exist in the glassy state at 296 K, the temperature of our diffusion measurement. Figure 6 also shows data from refs 6 and 21 for comparison. There are significant differences (as large as 20 K) between the data from this work and ref 6. Because we report the onset T_g and ref 6 reports the midpoint, the disagreement is even greater. Scatter of this magnitude has been reported for other disaccharide−water systems.[22,23] In the case of maltose−water, we attribute the disagreement in T_g to the disagreement in water concentrations, especially at low values. The ref 6 study used loss-on-vacuum-drying at 333 K over P_2O_5 to obtain water concentrations. In contrast, our study used KF titration to measure water concentrations. By dissolving a sample in the KF reagent, this procedure ensures that all water is measured, including the portion tenaciously bound. It is our experience that drying at 333 K is insufficient for removing all water in maltose in practical times, and temperatures as high as 393 K are necessary for complete drying.

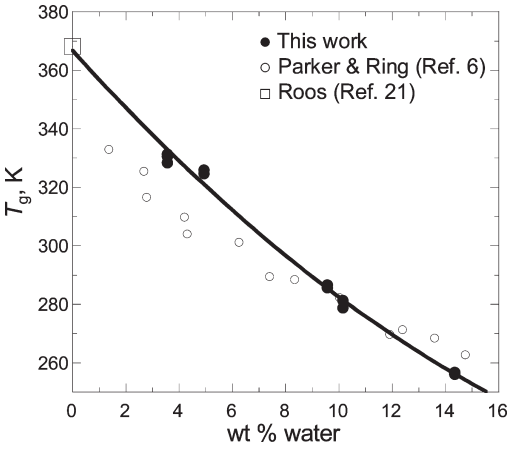

Figure 6. The glass transition temperature T_g of a maltose−water solution vs water concentration. Data are from this work and refs 6 and 21. All values are onset temperatures of the glass transition, except for those from ref 6, which are midpoints.

Crystalline maltose monohydrate contains only the β anomer,[24] whereas the aqueous solution of maltose contains a mixture of α and β anomers at equilibrium.[25] Because anomers have different physical properties, it is pertinent to specify the anomeric composition for the maltose matrix in which water diffusion has been measured. In previous studies, the anomeric composition was unspecified[6,7] or taken to be the α only.[11] We confirmed by NMR that our raw material crystalline maltose monohydrate contained only the β anomer. We did so by dissolving the material in dimethyl sulfoxide (DMSO) and measuring its spectrum immediately. In comparison, the water−maltose solutions prepared for diffusion measurements showed an anomeric ratio of approximately 60:40 (β/α), which is consistent with a literature value for the equilibrium anomeric ratio.[25] This ratio was achieved relatively quickly; for example, it was obtained after preparing a 50 wt % solution by dissolving the components at 333 K.

DISCUSSION

We have used Raman microscopy and isotope labeling to measure water self-diffusion in amorphous carbohydrates. Together with NMR, this method has yielded water diffusion coefficient D_w in water−maltose solutions over 8 orders of magnitude, from the liquid to the glassy state. Below we compare our data with the literature data to evaluate the new method and to extract systematic trends for diffusion in amorphous carbohydrates.

Agreement between Experimental Data on Diffusion in Water−Disaccharide Solutions. Figure 7a compares the self-diffusion coefficients of water D_w from this work and the literature[2−4,6,7] for water−disaccharide solutions near the ambient temperature (296−303 K). For NMR-derived D_w values (>10^{-11} m^2/s), there is consistency between various studies not only for the water−maltose system (compare this work and ref 3) but also for all water−disaccharide systems for which data exist. The value of D_w at the same concentration is insensitive to the identity of the disaccharide (sucrose, trehalose, or maltose) and to a slight change of temperature from 298 to 303 K.

For $D_w < 10^{-11}$ m^2/s, our results from Raman measurements at 296 K are compared with those from the evaporative-drying

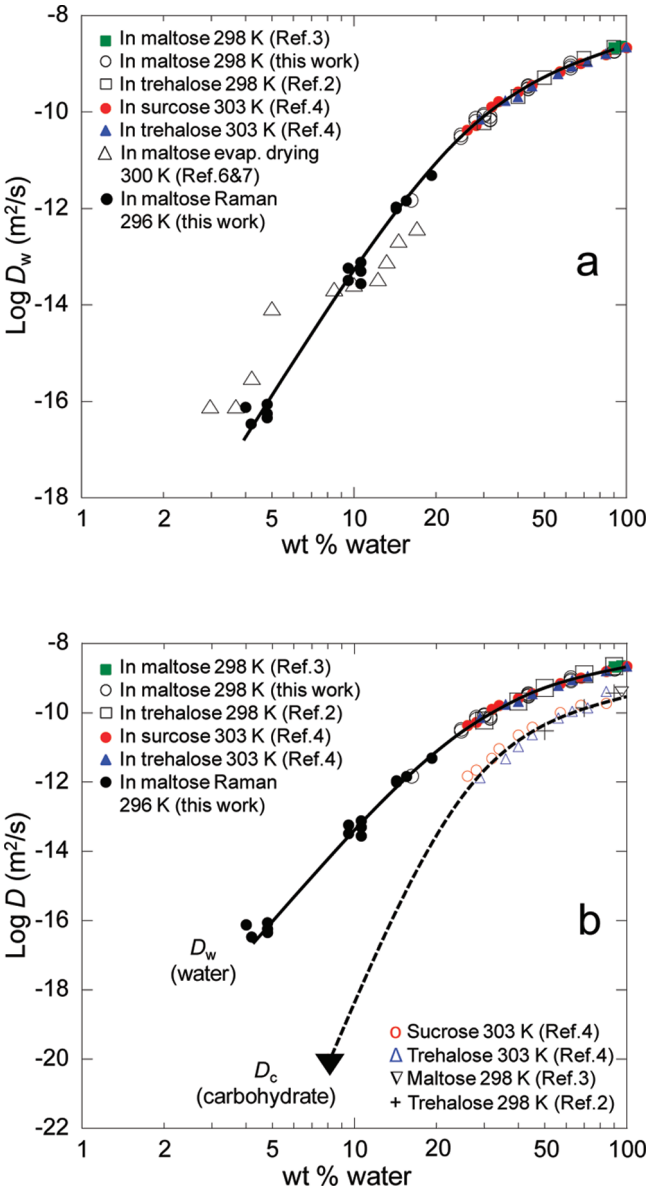

Figure 7. (a) Comparison of water diffusion coefficients in water−disaccharide solutions from this and previous studies.[2−4,6,7] T = 296−303 K. (b) Comparison of water and disaccharide diffusion coefficients in water−disaccharide solutions at 296−303 K. ▼indicates the estimated D for disaccharide molecules in a water−disaccharide solution at T_g.

measurements at 300 K.[6,7] Our values are higher than previous values in the concentration range 15−20 wt % water, but lower at lower water concentrations. Furthermore, the previous data show breaks in the D_w versus water concentration plot, whereas our data do not. Our data appear to correlate better with the NMR-derived D_w values than the previous data. Below we consider the possible reasons for these differences, including accuracy of water concentration, effect of surface dehydration during vacuum drying, and water diffusion versus proton exchange.

(1) Accuracy of water concentration. Water concentrations were determined by Karl Fisher titration in this study, and by vacuum drying at 333 K in the previous studies.[6,7] As we argue in the context of Figure 6, this drying condition may be insufficient for removing all water from the sugar matrix and lead to underestimated water concentrations. If the water concentrations in refs 6 and 7 are recalculated by equating their T_g values with ours (Figure 6), the disagreement shown in Figure 7a between the D_w values of this and previous studies is significantly reduced. The revised water concentrations would also diminish the breaks in the D_w versus water concentration plots reported in refs 6 and 7.

(2) Effect of surface dehydration during vacuum drying. A potential difficulty with the evaporative drying method exists when diffusion rate depends strongly on concentration,[12] which is the case for water diffusing in amorphous carbohydrates (Figure 7a). During evaporative drying, such systems are expected to develop dry surface layers in which diffusion is much slower. In this study we have indeed observed this phenomenon. For example, a droplet of maltose−water solution with 15 wt % water changed from clear to cloudy in minutes as it evaporated. This change was only at the surface because cutting the droplet open revealed a clear interior. For such systems, the D_w obtained by evaporative drying is a mean diffusion coefficient averaged over a range of concentrations, and careful corrections must be made to calculate diffusion coefficients at the concentrations of interest.[12] This difficulty is not encountered with our method because diffusion occurs in a medium of constant water concentration. Our measurement could be carried out to much longer time (weeks for samples of the lowest water concentrations) without observing significant deviation from Fickian kinetics.

(3) Water diffusion versus proton exchange. The evaporative drying method measures the diffusion of whole water molecules; the NMR and the Raman mapping method (configured to track proton diffusion) measure the migration of protons. In theory, protons can migrate through exchanges even if water molecules (oxygen atoms) remain stationary. Such proton migrations would be detectable by NMR and Raman, but not by evaporative drying. Thus, if water diffusion and proton exchange occur simultaneously, NMR and Raman microscopy would report faster water diffusion than evaporative drying. Since this is generally not the case (Figure 7a), we conclude that the NMR and Raman methods do measure whole-molecule diffusion of water.

Water Diffusion versus Carbohydrate Diffusion. Although our study did not measure the diffusion of maltose, we have plotted in Figure 7b the diffusion coefficients D_c of disaccharides (sucrose, trehalose, and maltose) in aqueous solutions,[2−4] so that a comparison is possible with water diffusion coefficients in the same solutions. At our scale of comparison, D_c, like D_w, is not strongly dependent on the identity of the disaccharide or a slight change of temperature from 298 to 303 K.

Figure 7b shows that $D_w/D_c \approx 10$ at high water concentrations, and that this ratio increases with decreasing water concentration. This comparison of D_w and D_c is possible down to 30 wt % H_2O with the NMR data. To extend this comparison to still lower water concentrations, we estimate the value of D_c at 8 wt % water, at which a maltose−water solution at 296 K undergoes the glass transition. For this purpose, we note that (*i*) $D \approx 10^{-20}$ m²/s for a one-component organic liquid at T_g;[26,27] (*ii*) $D \approx 10^{-18}$ m²/s for fluorescein diffusing in a sucrose−water solution

dx.doi.org/10.1021/jp202663r |J. Phys. Chem. B 2011, 115, 5849–5855

containing 10 wt % water at T_g;[28] and (*iii*) $D \approx 10^{-23}$ m^2/s (estimated by extrapolation) for fluorescein diffusing in sucrose−water solutions at T_g containing more than 15 wt % water.[28] Taking 10^{-20} m^2/s as an estimate for D_c at T_g (lowest symbol, Figure 7b), we obtain $D_w/D_c = 10^6$ at T_g, which indicates that water diffusion is strongly decoupled from and enhanced over matrix diffusion in carbohydrate glasses.

The increasing D_w/D_c ratio with decreasing water concentration (Figure 7b) is qualitatively similar to the decoupling phenomenon observed in other systems: water in polymers,[12,29] fast ions in glasses,[30] small-molecule dyes in PS,[31] and more. In all these systems, diffusion of certain species remains remarkably fast even as the system is vitrified and the decoupling of diffusion is more pronounced as the glass transition is approached from above. For water−carbohydrate systems, computational studies have considered the possibility that water molecules diffuse by different mechanisms (e.g., by translational jumps) from carbohydrate molecules.[4,9,10] If this is the case, decoupling between water and carbohydrate diffusion would not be surprising.

CONCLUSIONS

We have used Raman microscopy and isotope labeling for the first time to measure the water self-diffusion coefficient D_w in carbohydrate glasses. Together with NMR, this method allowed measurement of D_w in amorphous maltose over 8 orders of magnitude, from the liquid to the glassy state. We find significant differences between our results and those from evaporative drying, but the discrepancy might be in part due to the accuracy of water concentrations. Our data show that water self-diffusion is remarkably fast in maltose glasses, decouples from maltose diffusion, and is not strongly affected by the glass transition. These findings are relevant for understanding water diffusion in carbohydrates and for predicting the rate of hydration and the stability of amorphous food, drugs, and biomaterials.

For water−disaccharide solutions studied to date, the water diffusion rate is weakly dependent on the identity of the disaccharide down to a water concentration of 30 wt %. It would be of interest to determine whether such "master-curve" behavior persists at even lower water concentrations and into the glassy state. Answering this question is relevant for assessing the effectiveness of different carbohydrate matrices for stabilizing proteins and cells, for which trehalose has been suggested to be special. Including mono- and polysaccharides in this analysis could help understand the effect of carbohydrate molecular weight on water diffusion.

This study demonstrates the utility of Raman microscopy for measuring water diffusion in solid matrices. For diffusion measurements, the spatial resolution of Raman microscopy (ca. 1 μm) is modest in comparison with such techniques as secondary ion mass spectroscopy. This technique, however, is useful for bridging the high-resolution methods and the standard "liquid diffusion" methods such as NMR. Raman microscopy is relatively available, nondestructive, and able to distinguish complex molecules.

AUTHOR INFORMATION

Corresponding Author

*Tel.: (608)263-2263; e-mail: lyu@pharmacy.wisc.edu.

Present Addresses

[§]Biopharmaceutics R&D, Bristol-Myers Squibb Company, New Brunswick, NJ 08903.

ACKNOWLEDGMENT

We thank USDA (Grant 2005-01303), NSF (DMR 0907031), and Thermo Fisher Scientific for supporting this work, the Analytical Instrumentation Center of the School of Pharmacy, UW-Madison, for support in obtaining NMR data, and Richard Hartel and M. D. Ediger for helpful discussions.

REFERENCES

(1) Moran, G. R.; Jeffrey, K. R. *J. Chem. Phys.* **1999**, *110*, 3472–3483.
(2) Rampp, M.; Buttersack, C.; Ludemann, H.-D. *Carbohydr. Res.* **2000**, *328*, 561–572.
(3) Engelsen, S. B.; Monteiro, C.; de Penhoat, C. H.; Perez, S. *Biophys. Chem.* **2001**, *93*, 103–127.
(4) Ekdawi-Sever, N.; de Pablo, J. J.; Feick, E.; von Meerwall, E. *J. Phys. Chem. A* **2003**, *107*, 936–943.
(5) Branca, C.; Magazù, S.; Maisano, G.; Telling, M. T. F. *J. Phys. Chem. B* **2004**, *108*, 17069–17075.
(6) Parker, R.; Ring, S. G. *Carbohydr. Res.* **1995**, *273*, 147–155.
(7) Tromp, R. H.; Parker, R.; Ring, S. G. *Carbohydr. Res.* **1997**, *303*, 199–205.
(8) Aldous, B. J.; Franks, F.; Greer, A. L. *J. Mater. Sci.* **1997**, *32*, 301–308.
(9) Roberts, C. J.; Debenedetti, P. G. *J. Phys. Chem. B* **1999**, *103*, 7308–7318.
(10) Molinero, V.; Goddard, W. A., III *Phys. Rev. Lett.* **2005**, *95*, 045701.
(11) Limbach, H. J.; Ubbink, J. *Soft Matter* **2008**, *4*, 1887–1898.
(12) Crank, J.; Park, G. S. In *Diffusion in Polymers*; Academic Press Inc.: London, 1967.
(13) Friedman, I.; Long, W. *Science* **1976**, *191*, 347–352.
(14) Everall, N. *Appl. Spectrosc.* **2000**, *54*, 773–1515.
(15) Bridges, T. E.; Uibel, R. H.; Harris, J. M. *Anal. Chem.* **2006**, *78*, 2121–2129.
(16) Stejskal, E. O.; Tanner, J. E. *J. Chem. Phys.* **1965**, *42*, 288–292.
(17) Tanner, J. E. *J. Chem. Phys.* **1970**, *52*, 2523–2526.
(18) Holz, M.; Weingärtner, H. *J. Magn. Reson.* **1991**, *92*, 115–125.
(19) *Scientist*, version 3.0; MicroMath, Inc.: St. Louis, MO, 2005 (http://www.micromath.com/)
(20) Winchell, A. N. *The Optical Properties of Organic Compounds*, 2nd ed., McCrone Research Institute: Chicago, IL, 1987.
(21) Roos, Y. *Carbohydr. Res.* **1993**, *238*, 39–48.
(22) Frank, G. A. *J. Phys. Chem. Ref. Data* **2007**, *36*, 1279–1285.
(23) Chen, T.; Fowler, A.; Toner, M. *Cryobiology* **2000**, *40*, 277–282.
(24) Quigley, G.. J.; Sarko, A.; Marchessault, R. H. *J. Am. Chem. Soc.* **1970**, *92*, 5834–5839.
(25) Bekiroglu, S.; Kenne, L.; Sandström, C. *J. Org. Chem.* **2003**, *68*, 1671–1678.
(26) Mapes, M. K.; Swallen, S. F.; Ediger, M. D. *J. Phys. Chem. B* **2006**, *110*, 507–511.
(27) Swallen, S. F.; Traynor, K.; McMahon, R. J.; Ediger, M. D.; Mates, T. E. *J. Phys. Chem. B* **2009**, *113*, 4600–4608.
(28) Champion, D.; Hervet, H.; Blond, G.; Le Meste, M.; Simatos, D. *J. Phys. Chem. B* **1997**, *101*, 10674–10679.
(29) Oksanen, C. A.; Zografi, G. *Pharm. Res.* **1993**, *10*, 791–799.
(30) Angell, C. A. *Chem. Rev.* **1990**, *90*, 523–542.
(31) Cicerone, M. T.; Blackburn, F. R.; Ediger, M. D. *Macromolecules* **1995**, *28*, 8224–8232.